Finite-Time Distributed Leaderless Cooperative Guidance Law for Maneuvering Targets under Directed Topology without Numerical Singularities

Xiaofei Dong [1,2,*] **and Zhang Ren** [1]

1 School of Automation Science and Electrical Engineering, Beihang University, Beijing 100191, China; renzhang@buaa.edu.cn
2 Science and Technology on Complex System Control and Intelligent Agent Cooperation Laboratory, Beijing 100074, China
* Correspondence: dxf891112@126.com

Abstract: A new distributed leaderless cooperative guidance algorithm is suggested for multi-directional saturation strikes against maneuvering targets. First, the finite-time disturbance observer (FDO) is used to estimate the target's unknown maneuvers. After that, the guidance laws along the line-of-sight (LOS) direction and the LOS normal direction are designed separately based on the finite-time consensus theory. The proposed guidance law could satisfy both impact time and LOS angle constraints. Numerical singularities due to feedback linearization are avoided by nonlinear stability analysis. Finally, the effectiveness of the proposed cooperative guidance law is proved by numerical simulation arithmetic.

Keywords: distributed cooperative guidance; maneuvering targets; finite-time consensus

1. Introduction

In the last decade, cooperative guidance has received significant attention for its effectiveness in increasing the rate of defense penetration and aircraft-target interception. Well-coordinated multiple vehicles tend to be more efficient. They can raise the effectiveness of defense penetration by attacking the target from numerous different directions simultaneously. Cooperative guidance against maneuvering targets allows for a multi-vehicle-to-target interception posture. As a result, the target's cost of maneuvering to escape increases, and the interception success rate improves.

The cooperative guidance law can be functionally divided into impact angle cooperation and impact time cooperation. The information exchanged between the vehicles was not considered in the initial study. Instead, the cooperative attack was achieved through predefined impact angles and impact times [1–4]. The limitation of this method is that it is difficult to find reasonable predetermined values. If the time and angle of impact are not set properly, there is a risk of increasing energy consumption and even resulting in guidance failure.

The current research focuses on cooperative guidance. The remaining flight time and impact angle are selected as coordination variables. Then the distributed cooperative guidance law (DCGL) was established by local communication based on consensus theory. Among the existing literature on cooperative guidance, the most extensive research has been conducted on cooperative time-coordinated guidance against a stationary target [5–11]. Wang, et al. [5] proposed a two-step guidance algorithm. At the first step, a DCGL was developed based on the consensus theory of the second-order system. During the second step, a simultaneous attack was achieved using a proportional guidance method. Zhao, et al. [6] proposed a new cooperative guidance method that reduces the computational effort by triggering only at a specific time. Jiang, et al. [7] simultaneously attacking

with multiple constraints was realized based on the backward horizon control (RHC) algorithm. Zhang, et al. [8] investigated the issue of optimal DCGL for stationary targets under directed topologies. A two-stage guidance method was developed to optimize energy consumption while ensuring simultaneous collision against the target. Chen, et al. [9] proposed a cooperative guidance law for a vehicle with thrust control. This guidance law enables a coordinated attack under a hit angle constraint considering the velocity constraint. Li, et al. [10] investigated the issue of simultaneous arrival of multiple interceptors with effective partial actuators. A fault-tolerant cooperative guidance method was proposed, where an adaptive method was devised to handle uncertainties. Simultaneous arrivals within a fixed time interval under actuator failure conditions were achieved. Teng, et al. [11] suggested a new cooperative guidance method that achieves simultaneous hits in multiple directions without radial velocity measurement.

Currently, there are limited results of cooperative guidance for maneuvering targets [12–26]. Nikusokhan, et al. [12], it was hypothesized that the linearization condition of the engagement dynamics could be satisfied. The measurement information of the target acceleration, which is difficult to obtain, is directly used in [12–18]. Wang, et al. [19] presented a three-dimensional DCGL for several vehicles to strike a maneuvering target at predetermined impact angles. Yu, et al. [20] studied the design and analysis of DCGL against maneuvering targets. An extended state observer is first utilized to evaluate the target's maneuver. On this basis, a cooperative guidance law that enables a head-on saturation attack is proposed based on the leader-follower model. Wang, et al. [21] proposed a DCGL for hypersonic vehicles that solves the simultaneous arrival problem in the presence of uncontrollable velocity. Chen, et al. [22] proposed a three-dimensional nonlinear DCGL that enables multiple vehicles to simultaneously attack a maneuvering target at a predetermined LOS angle. Liu, et al. [23] investigated robust differential games and their application in cooperative guidance. The suggested guidance method is able to avoid input saturation while synchronizing arrival times.

At present, the following problems still exist with cooperative guidance for maneuvering targets. The first issue is how to estimate the maneuver of the target. In [12–17] need to obtain the acceleration of the target directly, which is usually difficult to measure directly by sensors. In the literature [20,21], it also needs to be assumed that the target acceleration is constant or slowly varying. The second problem is the large tangential acceleration command for the vehicle. In the literature [24,25], the acceleration signal is made singular at the end of the guidance due to the feedback linearization method. In practice, the tangential acceleration of the aircraft cannot respond to excessive commands. In the literature [19,22,26], both the missile-target distance and the rate of the distance are needed to achieve consensus. This is unnecessary and could lead to larger energy consumption. Finally, in terms of communication topology, the approach in the literature [18] is centralized, while the approach in the literature [19,22,24,25] can only be applied to undirected topologies.

This paper investigates the cooperative guidance issue for maneuvering targets and proposes a new guidance law with the following advantages:

1. The suggested guidance strategy could be used for the maneuvering target. At the same time, the guidance method does not need direct access to the acceleration measurement information of the target and does not need the acceleration of the target to be constant or slowly varying.

2. The design and analysis of the guidance law are conducted directly on the nonlinear model, avoiding the disadvantages of numerical singularities and excessive guidance commands due to feedback linearization. It is also shown that the guidance law is finite-time converged based on the homogeneous system stability theory.

3. The proposed guidance method is distributed and only requires neighborhood information. At the same time, he suggested that the method can be used to a directed communication topology through a rigorous stability analysis.

The rest of the paper is structured as follows. In Section 2, some necessary preliminaries are presented. In Section 3, the studied cooperative guidance problem is described. In Section 4, the major results, including the design of the distributed guidance algorithm and the stability analysis, are elaborated. In Section 5, the simulation verification on the proposed distributed guidance algorithm is performed. Lastly in Section 6, conclusions are drawn.

2. Preliminaries

Lemma 1. *Under Assumption 1, there exists a positive column vector* $\theta = (\theta_1, \ldots, \theta_N)^{\mathrm{T}}$ *such that* $\theta_i a_{ij} = \theta_j a_{ji}$ *for all* $i, j = 1 \ldots, N$. *Denote* $\Theta = \mathrm{diag}(\theta_1, \ldots, \theta_N)$. *Then, the matrix* $\Theta \mathcal{L}$ *is symmetric.*

Lemma 2. [27] *Consider the system*

$$\dot{x}(t) = f(t, x(t)), \ x(0) = x_0. \tag{1}$$

Assume that there is a continuous positive definite function $V(x) : \mathcal{D} \to \mathbb{R}$ *for any real number* $c > 0$ *and* $\alpha \in (0, 1)$, *the following inequality holds*

$$\dot{V}(x) + cV^{\alpha}(x) \leq 0, \ x \in \mathcal{N} \backslash \{0\}. \tag{2}$$

Then, the origin is a finite-time stable equilibrium of (1), and the settling time is

$$T(x_0) \leq \frac{1}{c(1-\alpha)} V^{(1-\alpha)}(x_0). \tag{3}$$

Lemma 3. [28] *Let* $\xi_1, \xi_2, \ldots, \xi_N \geq 0$ *and* $0 < p \leq 1$. *Then*

$$\sum_{i=1}^{N} \xi_i^p \geq \left(\sum_{i=1}^{N} \xi_i \right)^p. \tag{4}$$

Definition 1. *Select the following system*

$$\dot{x} = f(x), \ f(0) = 0, \ x(0) = x_0, \ x \in \mathbb{R}^m \tag{5}$$

where $f(x) = [f_1(x), f_2(x), \cdots, f_m(x)]^T : U_0 \to \mathbb{R}^m$ *is a continuous vector field in an open neighborhood* U_0 *around the origin. Let* $(r_1, r_2, \cdots, r_m) \in \mathbb{R}^m$ *with* $r_i > 0$, $i = 1, 2, \cdots, m$. $f(x)$ *is called homogeneous of degree* $\kappa \in \mathbb{R}$ *with respect to* $(r_1, r_2, \cdots, r_m)$ *if for any given* $\varepsilon > 0$, $f_i(\varepsilon^{r_1} x_1, \varepsilon^{r_2} x_2, \cdots, \varepsilon^{r_m} x_m) = \varepsilon^{\kappa + r_i} f_i(x)$, $i = 1, 2, \cdots, m$, $\forall x \in \mathbb{R}^m$. *System (5) is called homogeneous if* $f(x)$ *is homogeneous.*

Lemma 4. *Consider system (5) with* $f(x)$ *as a continuous homogeneous vector field of degree* $\kappa < 0$ *with respect to* $(r_1, r_2, \cdots, r_m)$. *If the system (5) is globally asymptotically stable, for any initial,* $x(0) \in \mathbb{R}^m$ *it converges to origin in finite time.*

3. Problem Description

In this section, the problem of cooperative guidance is described. The problem we consider is that several unmanned aerial vehicles (UAVs) attack a target in an arbitrary maneuver. The following is a typical assumption when considering cooperative guidance problems in engineering practice.

The following assumptions are given:

Assumption 1. *The topology of directed communication between agents is strongly connected and detail balanced.*

Assumption 2. *The disturbance satisfies the following conditions:*

$$\begin{aligned} |\dot{w}_{ri}| &\leq w_1 \\ |\dot{w}_{qi}| &\leq w_2 \end{aligned} \tag{6}$$

where w_{ri} and w_{qi} denote the disturbance caused by the target maneuver in the direction of the line of sight and the component normal to the line of sight, respectively. Meanwhile w_1 and w_2 are known constants respectively.

Assumption 3. *The seeker and autopilot dynamics of the missiles are fast enough in comparison with the guidance loop.*

The geometric relationships in the guidance process are illustrated in Figure 1 where m_i denotes the i th UAV, and T denotes the target.
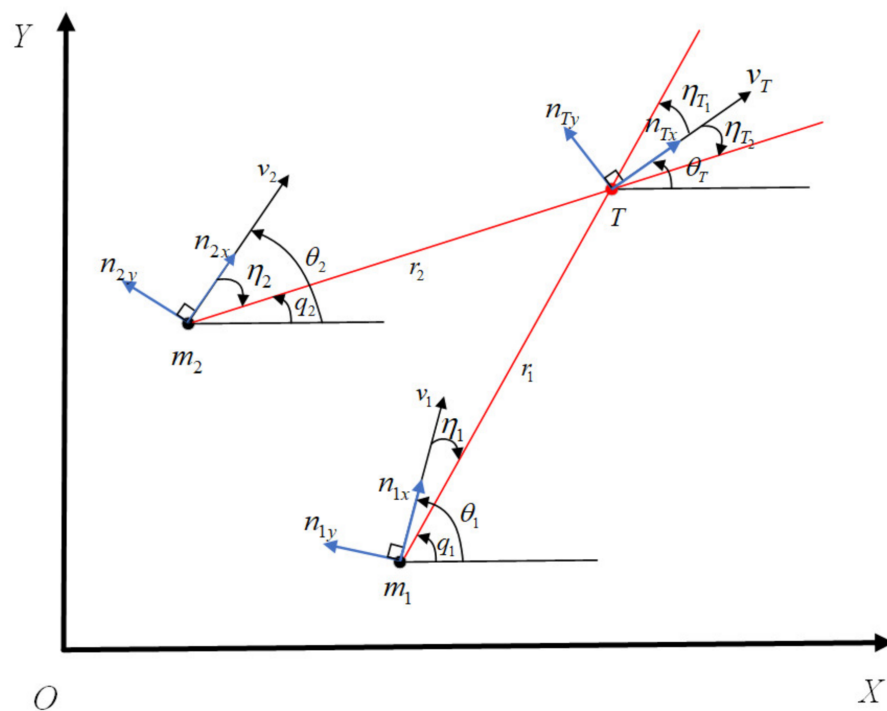
Figure 1. The geometric relationship between multiple UAVs and targets.

The terms q_i, η_i, θ_i stand for the LOS angle, leading angle, flight path angle, respectively. From the geometric relations in Figure 1, we can obtain that

$$\eta_i = q_i - \theta_i. \tag{7}$$

We note that a case $\eta_i \in [0, -\pi]$, (i.e., $\theta_i(t) \geq q_i(t)$) can be considered as an asymmetry of a case $\eta_i \in [0, \pi]$, (i.e., $\theta_i(t) \leq q_i(t)$). The case $\eta_i(t) \in [0, \pi]$ is treated in this paper. The case pursued is made by

$$\begin{cases} \dot{r}_i = V_T \cos \eta_{Ti} - V_i \cos \eta_i \\ r_i \dot{q}_i = V_i \sin \eta_i - V_T \sin \eta_{Ti} \\ \dot{\theta}_i = n_{iy}/V_i \\ \dot{V}_i = n_{ix} \end{cases} \tag{8}$$

where r_i is the distance from m_i to the target; V_i represents the velocity of m_i, while n_{ix} as well as n_{iy} are the overloads of m_i in its velocity frame, tuning the magnitude and direction of V_i, and η_{Ti}, V_T stands for the leading angle and the velocity of the target.

Taking the derivative of $\dot{r}_i$ we can obtain that

$$
\begin{aligned}
\ddot{r}_i &= \dot{V}_T \cos \eta_{Ti} - V_T \sin \eta_{Ti} \dot{\eta}_{Ti} - \dot{V}_i \cos \eta_i + V_i \sin \eta_i \dot{\eta}_i \\
&= \dot{V}_T \cos \eta_{Ti} + V_T \sin \eta_{Ti} \dot{\theta}_T - \dot{V}_i \cos \eta_i - V_i \sin \eta_i \dot{\theta}_i + r_i \dot{q}_i{}^2.
\end{aligned}
$$

Denote that

$$
\begin{aligned}
w_{ri} &= \dot{V}_T \cos \eta_{Ti} + V_T \sin \eta_{Ti} \cdot \dot{\theta}_T \\
u_{ri} &= \dot{V}_i \cos \eta_i + V_i \sin \eta_i \dot{\theta}_i
\end{aligned}
$$

then we can obtain further

$$
\ddot{r}_i = w_{ri} - u_{ri} + r_i \dot{q}_i{}^2. \tag{9}
$$

The remaining flight time t_{goi} of the vehicle can be roughly estimated as

$$
t_{goi} = -\frac{r_i}{\dot{r}_i}. \tag{10}
$$

Taking the derivative of (10) and substituting (9) we can obtain

$$
\dot{t}_{goi} = -1 + \frac{r_i^2 \dot{q}_i^2}{\dot{r}_i^2} - \frac{r_i}{\dot{r}_i^2} u_{ri} + \frac{r_i}{\dot{r}_i^2} w_{ri}. \tag{11}
$$

Taking the derivative of $\dot{q}_i$, we can obtain

$$
\begin{aligned}
\ddot{q}_i &= \frac{1}{r_i^2} \cdot (r_i(t) \cdot (\dot{V}_i \sin \eta_i + V_i \cos \eta_i \dot{\eta}_i - \dot{V}_T \sin \eta_{Ti} \\
&\quad - V_T \cos \eta_{Ti} \dot{\eta}_{Ti}) - r_i \dot{r}_i \dot{q}_i).
\end{aligned}
$$

Denote that

$$
w_{qi} = \dot{V}_T \sin \eta_{Ti} - V_T \cos \eta_{Ti} \cdot \dot{\theta}_T
$$

and

$$
u_{qi} = \dot{V}_i \sin \eta_i - V_i \cos \eta_i \cdot \dot{\theta}_i.
$$

Note that $\dot{\eta}_i = \dot{q}_i - \dot{\theta}_i$, and $\dot{\eta}_{Ti} = \dot{q}_i - \dot{\theta}_T$ then we can get

$$
\ddot{q}_i = \frac{1}{r_i}(u_{qi} - w_{qi}) - 2 \cdot \frac{\dot{q}_i \cdot \dot{r}_i}{r_i}. \tag{12}
$$

Illustrative Example. The purpose of the cooperative attack is to enable multiple UAVs to achieve a simultaneous attack on the target while ensuring their cooperation in terms of hitting angles. Simultaneous strikes can be achieved if and only if the remaining flight time achieves consensus. From (10), we can find that the remaining flight time of the UAV is determined by r_i and $\dot{r}_i$. At the same time, we can see that if $\lim_{t \to T_{end}} \dot{q}_i = 0$ then the UAV m_i is able to hit the target. Then we are able to obtain the following definition.

Definition 2. *If the following equations hold simultaneously, the multi-UAVs system achieves a coordinated attack in finite time.*

$$
\begin{cases}
\lim\limits_{t \to T_{end}} ((q_i - c_i) - (q_j - c_j)) = 0 \\
\lim\limits_{t \to T_{end}} \dot{q}_i = \lim\limits_{t \to T_{end}} \dot{q}_j = 0 \qquad \forall i, j \in N \\
\lim\limits_{t \to T_{end}} (t_{goi} - t_{goj}) = 0
\end{cases} \tag{13}
$$

where c_i and c_j are default constants and T_{end} is a limited adjustment time.

4. Main Result

This section proposes a sliding-mode FDO to evaluate the interference caused by target maneuvers in finite time. After that, based on the finite-time consensus theory, u_{ri} and u_{qi} are designed to enable simultaneous multi-directional attacks against the target, respectively.

4.1. FDO Design

Inspired by [29], the FDO is designed as

$$
\begin{cases}
\dot{\hat{w}}_{qi} = \alpha \widetilde{w}_{qi}^{2-\frac{p}{q}} + \beta \widetilde{w}_{qi}^{\frac{p}{q}} + w_1 \mathrm{sgn}|\widetilde{w}_{qi}| \\
\dot{\hat{w}}_{ri} = \alpha \widetilde{w}_{ri}^{2-\frac{p}{q}} + \beta \widetilde{w}_{ri}^{\frac{p}{q}} + w_2 \mathrm{sgn}|\widetilde{w}_{ri}|
\end{cases}
\tag{14}
$$

then the observation error are:

$$
\begin{cases}
\widetilde{w}_{qi} = w_{qi} - \hat{w}_{qi} = r_i(\ddot{q}_i - \frac{2\dot{q}_i}{t_{goi}} + \frac{1}{r_i}u_{qi}) - \hat{w}_{qi} \\
\widetilde{w}_{ri} = w_{ri} - \hat{w}_{ri} = \frac{\dot{r}_i}{x_{3i}}(-\dot{t}_{goi} - 1 + \dot{q}_i^2 t_{goi}^2 + \frac{t_{goi}}{r_i}u_{ri}) - \hat{w}_{ri}.
\end{cases}
\tag{15}
$$

Theorem 1. *If Assumption 2 holds, and the parameters satisfy that $\alpha > 0$, $\beta > 0$, $q > p > 0$, then the disturbance observation error $\widetilde{w}_{qi}$ and $\widetilde{w}_{ri}$ are able to converge in finite time.*

Proof of Theorem 1. Define the Lyapunov function as:

$$
V_{1i} = \frac{1}{2}\widetilde{w}_{qi}^2 + \frac{1}{2}\widetilde{w}_{ri}^2.
\tag{16}
$$

Taking the time derivative of the above function, we can get

$$
\begin{aligned}
\dot{V}_{1i} &= \widetilde{w}_{qi}\dot{\widetilde{w}}_{qi} + \widetilde{w}_{ri}\dot{\widetilde{w}}_{ri} \\
&= \widetilde{w}_{qi} \cdot (\dot{w}_{qi} - \alpha \widetilde{w}_{qi}^{2-\frac{p}{q}} - \beta \widetilde{w}_{qi}^{\frac{p}{q}} - w_1 \mathrm{sgn}|\widetilde{w}_{qi}|) \\
&\quad + \widetilde{w}_{ri} \cdot (\dot{w}_{ri} - \alpha \widetilde{w}_{ri}^{2-\frac{p}{q}} - \beta \widetilde{w}_{ri}^{\frac{p}{q}} - w_2 \mathrm{sgn}|\widetilde{w}_{ri}|) \\
&\leq \widetilde{w}_{qi} \cdot (-\alpha \widetilde{w}_{qi}^{2-\frac{p}{q}} - \beta \widetilde{w}_{qi}^{\frac{p}{q}} + w_1(1 - \mathrm{sgn}|\widetilde{w}_{qi}|)) \\
&\quad + \widetilde{w}_{ri} \cdot (-\alpha \widetilde{w}_{ri}^{2-\frac{p}{q}} - \beta \widetilde{w}_{ri}^{\frac{p}{q}} + w_2(1 - \mathrm{sgn}|\widetilde{w}_{ri}|)) \\
&\leq -\alpha(\widetilde{w}_{qi}^2)^{\frac{3q-p}{2q}} - \beta(\widetilde{w}_{qi}^2)^{\frac{p+q}{2q}} - \alpha(\widetilde{w}_{ri}^2)^{\frac{3q-p}{2q}} - \beta(\widetilde{w}_{ri}^2)^{\frac{p+q}{2q}}.
\end{aligned}
\tag{17}
$$

According to Lemma 3 we can obtain

$$
\begin{aligned}
\dot{V}_{1i} &\leq -2\alpha(V_{1i}^2)^{\frac{3q-p}{2q}} - 2\beta(V_{1i}^2)^{\frac{p+q}{2q}} \\
&= -2(\alpha V_{1i}^{\frac{q-p}{q}} + \beta)V_{1i}^{\frac{p+q}{2q}}.
\end{aligned}
\tag{18}
$$

We can obtain $\alpha V_{1i}^{(p-q)/q} > 0$ from $\alpha > 0$, $q > p > 0$ then (18) can be rewritten as:

$$
\dot{V}_{1i} \leq -2\beta V^{(p+q)/2p}.
\tag{19}
$$

According to the finite-time stability theory in Lemma 2, if $\alpha > 0$, $\beta > 0$, $q > p > 0$, we can obtain that $V_{1i} \to 0$ in a finite time T_1. By the structure of V_{1i} we can get that $\widetilde{w}_{qi} \to 0$ in a finite time T_1, where $T_1 \leq \frac{q}{\beta(q-p)}V^{\frac{q-p}{2q}}(0)$. $\square$

4.2. Impact Angle Cooperation Part

According to Definition 2, we get the purpose of impact angle cooperation is

$$\begin{aligned} &\lim_{t \to T_{end}} \left((q_i(t) - c_i) - (q_j(t) - c_j) \right) = 0 \\ &\lim_{t \to T_{end}} \dot{q}_i(t) = \lim_{t \to T_{end}} \dot{q}_j(t) = 0. \end{aligned} \tag{20}$$

This means that the purpose of the LOS angle cooperation is to make the LOS angles of different UAVs into a predefined sequence. The cooperative guidance law is also supposed to make the LOS angular rate of each UAV asymptotically equal to zero.

Let

$$\begin{cases} \theta_{1i} = q_i - c_i \\ \theta_{2i} = \dot{q}_i. \end{cases} \tag{21}$$

It follows from Equation (12) that its derivative satisfies

$$\begin{cases} \dot{\theta}_{1i} = \theta_{2i} \\ \dot{\theta}_{2i} = -2\frac{\dot{r}_i}{r_i}\theta_{2i} + \frac{1}{r_i}(u_{qi} - w_{qi}). \end{cases} \tag{22}$$

and the guidance law is designed as follows

$$\begin{aligned} u_{qi} &= 2_i\dot{r}_i\theta_{2i} + \hat{w}_{qi} \\ &+ r_i(k_1 \sum_{j=1}^{N} a_{ij}\text{sig}(\theta_{1i} - \theta_{1j})^{\alpha_1} + k_2\text{sig}(\theta_{2i})^{\alpha_2}). \end{aligned} \tag{23}$$

Lemma 5. *Under Assumption 1, there exists an appositive column vector* $\tau = (\varsigma_1, \varsigma_2, \ldots \varsigma_N)^{\text{T}}$, *such that* $\varsigma_i a_{ij} = \varsigma_j a_{ji}$ *for all* $i, j = 1 \ldots, N$. *Denote* $\varsigma = \text{diag}(\varsigma_1, \varsigma_2, \ldots \varsigma_N)$ *then the matrix* ςL *is symmetric.*

Theorem 2. *If the parameters in the guidance law (23) are satisfied* $k_1 > 0$, $k_2 > 0$, $0 < \alpha_1 < 1$, $\alpha_2 = \frac{2\alpha_1}{1+\alpha_1}$, *then the impact angle coordination condition (20) is achieved in finite-time* T_2.

Proof of Theorem 2. Substituting (23) into (22) yields

$$\begin{cases} \dot{\theta}_{1i} = \theta_{2i} \\ \dot{\theta}_{2i} = -\frac{\tilde{w}_{qi}}{r_i} - k_1 \sum_{j=1}^{N} a_{ij}\text{sig}(\theta_{1i} - \theta_{1j})^{\alpha_1} - k_2\text{sig}(\theta_{2i})^{\alpha_2}. \end{cases} \tag{24}$$

Let

$$\begin{cases} \xi_1 = M \cdot \theta_1 \\ \xi_2 = \theta_2 \end{cases} \tag{25}$$

with $\theta_1 = (\theta_{11}, \theta_{12}, \cdots, \theta_{1N})^{\text{T}}$, $\theta_2 = (\theta_{21}, \theta_{22}, \cdots, \theta_{2N})^{\text{T}}$ and $M = I - 1\chi^{\text{T}}$ of which $\chi^T = (\chi_1, \chi_2, \ldots, \chi_N)$ satisfies $\chi^{\text{T}}\mathcal{L} = 0$ and $\sum_{i=1}^{N} \chi_i = 1$. According to the algebraic properties of M, we have $\xi_1 = 0$ and $\xi_2 = 0$ if and only if $\theta_{11} = \theta_{12} = \cdots = \theta_{1N}, \theta_{21} = \theta_{22} = \cdots = \theta_{2N} = 0$ respectively. From (24) and (25) we obtain

$$\begin{cases} \dot{\xi}_1 = M\xi_2 \\ \dot{\xi}_2 = -k_1\text{sig}(L\xi_1)^{\alpha_1} - k_2\text{sig}(\xi_2)^{\alpha_2} + \tilde{w}_q \end{cases} \tag{26}$$

where $w_q = diag\left(\frac{\widetilde{w}_{q1}}{r_1}, \frac{\widetilde{w}_{q2}}{r_2}, \cdots, \frac{\widetilde{w}_{qN}}{r_N}\right)$. Consider a Lyapunov function candidate

$$V_2 = k_1 \int_0^{L\xi_1} \varsigma \text{sig}(s)^{\alpha_1} ds + \frac{1}{2} \xi_2^{\mathrm{T}} (\varsigma L) \xi_2 \tag{27}$$

where $\varsigma = \text{diag}(\varsigma_1, \varsigma_2, \ldots \varsigma_N) > 0$. Noting that $L\xi_1$ and $\text{sig}(L\xi_1)^{\alpha_1}$ have the same component sign, we are able to obtain $\int_0^{L\xi_1} \varsigma \text{sig}(s)^{\alpha_1} ds > 0$ for any $\xi_1 \neq 0$. Furthermore, from $\varsigma L = (\varsigma L)^{\mathrm{T}}$ we know that $\xi_2^{\mathrm{T}}(\varsigma L)\xi_2 > 0$ for any $\xi_2 \neq 0$. Therefore, we obtain V_2 as a positive definition. Then the time derivative of the above function yields

$$\begin{aligned}
\dot{V}_2 &= k_1 (L\dot{\xi}_1)^{\mathrm{T}} \varsigma \text{sig}(L\xi_1)^{\alpha_1} + \xi_2^{\mathrm{T}} \varsigma L \dot{\xi}_2 \\
&= k_1 \xi_2^{\mathrm{T}} L^{\mathrm{T}} \varsigma \text{sig}(L\xi_1)^{\alpha_1} - k_1 \xi_2^{\mathrm{T}} \varsigma L \text{sig}(L\xi_1)^{\alpha_1} - k_2 \xi_2^{\mathrm{T}} \varsigma L \text{sig}(\xi_2)^{\alpha_2} \\
&\quad + \xi_2^{\mathrm{T}} \varsigma L \widetilde{w}_q \\
&= -k_2 \xi_2^{\mathrm{T}} \varsigma L \text{sig}(\xi_2)^{\alpha_2} + \xi_2^{\mathrm{T}} \varsigma L \widetilde{w}_q.
\end{aligned} \tag{28}$$

From the definition of $\dot{q}_i$ in (8) and note that both V_i and V_T are bounded, we can get that ξ_2 is bounded in $[0, T_1)$. Note that $\widetilde{w}_q$ is also bounded in $[0, T_1)$ we can obtain that $\xi_2^{\mathrm{T}} \varsigma L w_q$ is bounded in $[0, T_1)$ and its upper bound is assumed to be $\overline{w}_q$. It follows from (28) that:

$$\dot{V}_2 \leq -k_2 \xi_2^{\mathrm{T}} \varsigma L \text{sig}(\xi_2)^{\alpha_2} + \overline{w}_q \leq \overline{w}_q. \tag{29}$$

Thus, V_2 is bounded in $[0, T_1)$. When $t \geq T_1$, we get that $\widetilde{w}_q = 0$. Then we can receive that

$$\dot{V}_2 \leq -k_2 \xi_2^{\mathrm{T}} \varsigma L \text{sig}(\xi_2)^{\alpha_2} \leq 0. \tag{30}$$

It can be seen that $\dot{V}_2 = 0$ implies $\xi_1 = \xi_2 = 0$. It can be seen from LaSalle's invariance theorem that the system (26) can reach globally asymptotically stable for its zero equilibrium.

Next, we will prove that the system dynamics have a negative degree of homogeneity. Let $\zeta = (\xi_{11}, \xi_{12}, \ldots, \xi_{1N}, \xi_{21}, \xi_{22}, \ldots, \xi_{2N})^{\mathrm{T}} \in \mathrm{R}^{2N}$ while the derivative of ζ is $\dot{\zeta} = f(\zeta)$. Consider the dilation $(s_1, \ldots s_1, s_2, \ldots s_2)$, $s_1 > 0$, $s_2 > 0$ and homogeneity κ then we can gain

$$\begin{aligned}
f_i(\varepsilon^{s_1}\xi_{11}, \ldots, \varepsilon^{s_1}\xi_{1N}, \varepsilon^{s_2}\xi_{21}, \ldots, \varepsilon^{s_2}\xi_{2N}) &= \varepsilon^{s_2}\xi_{2i} - \sum_{j=1}^{N} \chi_j \varepsilon^{s_2}\xi_{2j} \\
&= \varepsilon^{s_2}\left(\xi_{2i} - \sum_{j=1}^{N} \chi_j \xi_{2j}\right)
\end{aligned}$$

$$f_{N+i}(\varepsilon^{s_1}\xi_{11}, \ldots, \varepsilon^{s_1}\xi_{1N}, \varepsilon^{s_2}\xi_{21}, \ldots, \varepsilon^{s_2}\xi_{2N})$$
$$= -k_1 \frac{1}{r_i} \text{sig}\left(\sum_{i=1}^{N} a_{ij}(\varepsilon^{s_1}\xi_{1i} - \varepsilon^{s_1}\xi_{1j})\right)^{\alpha_1} - k_2 \frac{1}{r_i} \text{sig}(\varepsilon^{s_2}\xi_{2i})^{\alpha_2}.$$

We can find for every $\varepsilon > 0$ we have $f_i(\varepsilon^{s_1}\xi_1, \varepsilon^{s_2}\xi_2, \cdots, \varepsilon^{s_{2N}}\xi_{2N}) = \varepsilon^{\kappa+s_i} f_i(x)$, $i = 1, 2, \ldots, 2N$. By Lemma 4, we have $\kappa < 0$ holds by setting $0 < \alpha_1 < 1$, $\alpha_2 = \frac{2\alpha_1}{1+\alpha_1}$. According to Lemma 4, the system (26) can achieve global finite-time stability. Then the impact angle coordination condition (20) could be achieved in finite-time. We have completed the proof. $\square$

4.3. Impact Time Cooperation Part

By Definition 2, the goal of time cooperation is

$$\lim_{t \to T_{end}} (t_{goi} - t_{goj}) = 0. \tag{31}$$

According to this goal, we design time cooperative guidance law as

$$u_{ri} = \hat{w}_{ri} - k_3 \text{sig}(\sum_{j=1}^{N} a_{ij}(t_{goi} - t_{goj}))^{\alpha_3}. \tag{32}$$

Theorem 3. *If the parameters in the guidance law (32) are satisfied $k_3 > 0$, $0 < \alpha_3 < 1$, then the impact angle coordination condition (31) could be achieved in finite time.*

Proof of Theorem 3. Substituting (32) into the system (11) we get

$$\dot{t}_{goi} = -1 + \dot{q}_i^2 t_{goi}^2 - k_3 \frac{r_i}{\dot{r}_i^2} \sum_{j=1}^{N} a_{ij} \text{sig}(t_{goi} - t_{goj})^{\alpha_3} - \frac{t_{goi}}{\dot{r}_i} \widetilde{w}_{ri}. \tag{33}$$

Let $x = (t_{go1}, t_{go2}, \ldots, t_{goN})^{\text{T}}$ then (33) can be rewritten as

$$\dot{x} = -\mathbf{1} + \mathbf{\Phi} - k_3 r \text{sig}(Lx)^{\alpha_3} - \widetilde{w}_r \tag{34}$$

where $\mathbf{\Phi} = \text{diag}(\dot{q}_1^2 t_{go1}^2, \dot{q}_2^2 t_{go2}^2, \ldots, \dot{q}_N^2 t_{goN}^2)$, $w_r = (\frac{t_{go1}}{\dot{r}_1} \widetilde{w}_{r1}, \frac{t_{go2}}{\dot{r}_2} \widetilde{w}_{r2}, \ldots, \frac{t_{goN}}{\dot{r}_N} \widetilde{w}_{rN})$ and $r = \text{diag}(\frac{r_1}{\dot{r}_1^2}, \frac{r_2}{\dot{r}_2^2}, \ldots \frac{r_N}{\dot{r}_N^2})$. Let $\zeta = Mx$. According to the algebraic properties of M, we have $\zeta = 0$ if and only if $t_{go1} = t_{go2} = \cdots = t_{goN}$, respectively. Take the time derivative of the above function yields:

$$\dot{\zeta} = -k_3 r \text{sig}(L\zeta)^{\alpha_3} + M\mathbf{\Phi} - M\widetilde{w}_r. \tag{35}$$

Consider a Lyapunov function candidate $V_3 = \frac{1}{2} \zeta^T \varsigma L \zeta$. It is convenient to obtain that V_3 is positive definite. Its derivative along (35) satisfies

$$\dot{V}_3 = -k_3 \zeta^{\text{T}} \varsigma L M r \text{sig}(L\zeta)^{\alpha_3} - \zeta^{\text{T}} \varsigma L w_r + \zeta^{\text{T}} \varsigma L \mathbf{\Phi}. \tag{36}$$

Based on the definition of ζ and $\mathbf{\Phi}$, we are able to obtain that V_3 is bounded in $t \in [0, T_2)$. From Theorems 1 and 2, we are able to get $\widetilde{w}_r = 0$ and $\mathbf{\Phi} = 0$ in $t \geq T_2$. Then (36) can be reformulated as

$$\dot{V}_3 = -k_3 \zeta^{\text{T}} L^{\text{T}} \varsigma M r \text{sig}(L\zeta)^{\alpha_3}. \tag{37}$$

Notice that $r > 0$ while $L\zeta$ and $\text{sig}(L\zeta)^{\alpha_3}$ has the same sign component-wise, we can obtain $\dot{V}_3 \leq 0$ and it can be seen that $\dot{V}_3 = 0$ indicates that $\zeta = 0$. It can be seen from LaSalle's invariance theorem that the system (35) can reach globally asymptotically stable for its zero equilibrium.

Using the same analysis as in Theorem 2, we are able to obtain that the system (35) has a negative degree of homogeneity when $0 < \alpha_3 < 1$. Then the impact time coordination condition (31) can be achieved in a finite time. □

Remark 1. *For comparison, it is helpful to review the literature's engagement models and guidance laws in References [24,25]. In Ref. [24] the derivative of t_{go} is given as:*

$$\dot{t}_{goi} = -1 + \frac{r_i^2 \dot{q}_i^2}{\dot{r}_i^2} - \frac{r_i}{\dot{r}_i^2} u_{ri}. \tag{38}$$

A three-dimensional version is given in the literature [25] as

$$\dot{t}_{go} = -1 + \frac{r_i^2}{\dot{r}_i^2}\dot{q}_\varepsilon^2 + \frac{r_i^2}{\dot{r}_i^2}\dot{q}_\beta^2 \cos^2 q_\varepsilon - \frac{r_i}{\dot{r}_i^2}u_{ri} + d_r. \tag{39}$$

By feedback linearization, the guidance law was designed in the literature [24,25] as

$$u_{ri} = r_i\dot{q}_i^2 - \frac{\dot{r}_i^2}{r_i}\tilde{u}_{ri} \tag{40}$$

and

$$u_{ri} = r_i\dot{q}_{\varepsilon i}{}^2 + r_i\dot{q}_{\beta i}{}^2 \cos^2 q_{\varepsilon i} - \frac{\dot{r}_i^2}{r_i}\tilde{u}_{ri} \tag{41}$$

$\dot{t}_{goi}$ can be rewritten as $\dot{t}_{goi} = -1 + \tilde{u}_{ri}$ in this way. References [24,25] designed consensus-based DCGL to achieve simultaneous arrival based on this model. However, the overload command has critical singularities when $r_i \to 0$. Due to the singularities, a_{ri} would diverge to infinity when $r_i \to 0$. The guidance law (32) does not use feedback linearization and therefore avoids singularities above.

5. Numerical Example

We verify the performance of the DCGL by a numerical example of attacking a maneuvering target by four UAVs. In which the speed of the target is 300 m/s. The target's normal acceleration is set to $20\cos(0.2t)\text{m/s}^2$. The communication topology of the vehicles is shown in Figure 2.
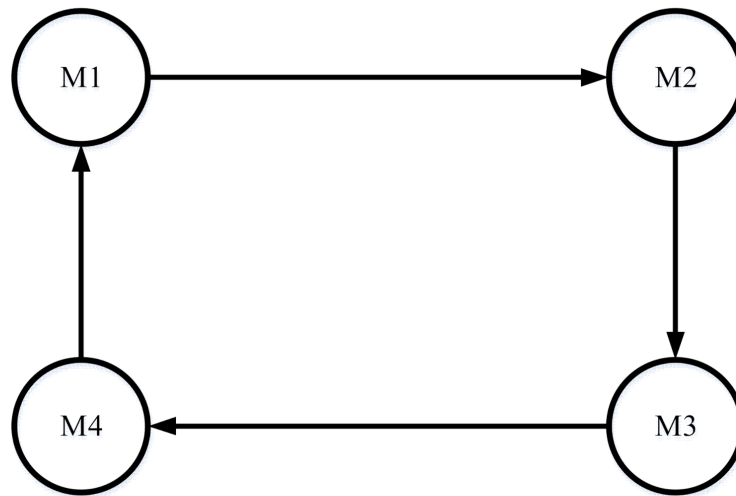
Figure 2. Communication topology among UAVs.

The initial conditions of multiple UAVs are shown in Table 1.

Table 1. Initial conditions of multiple UAVs.

UAV	Initial Position (m,m)	Initial Velocity/m/s	Heading Angle/°	Desired Angle/°
1	(0, −2000)	590	15	15
2	(0, −1000)	600	10	10
3	(0, 1000)	610	−10	5
4	(0, 2000)	590	−15	0

For the FDO, the parameters are set to be $\alpha = 1$, $\beta = 1$, $p = 1$, $q = 2$, $w_1 = w_2 = 10$. The parameters of the guidance law in the normal direction of LOS are set as $k_1 = 0.5$, $k_2 = 0.08$, $\alpha_1 = 0.5$, $\alpha_2 = 0.667$. Further, the guidance law parameters for the LOS direction are chosen as $k_3 = 2$, $\alpha_3 = 0.5$.

5.1. Simulation of Pursuit and Head-On Attacks

We set up two sets of simulations, where group A is a chase attack and group B is a head-on attack. The initial position of the target in group A is (12,000, 0) and the initial orientation is the initial heading angle of the target is $0°$. Group B target's initial position is (25,000, 0) the initial heading angle of the target is $180°$.

The simulation curves of the suggested cooperative guidance law, including the trajectories of the vehicles and the target, time-to-go of four UAVs to attack a maneuvering target, impact angle, LOS angular rate, radial relative velocities, actual and estimated values of external disturbance, and tangential and normal acceleration command, are shown in Figures 3–10.
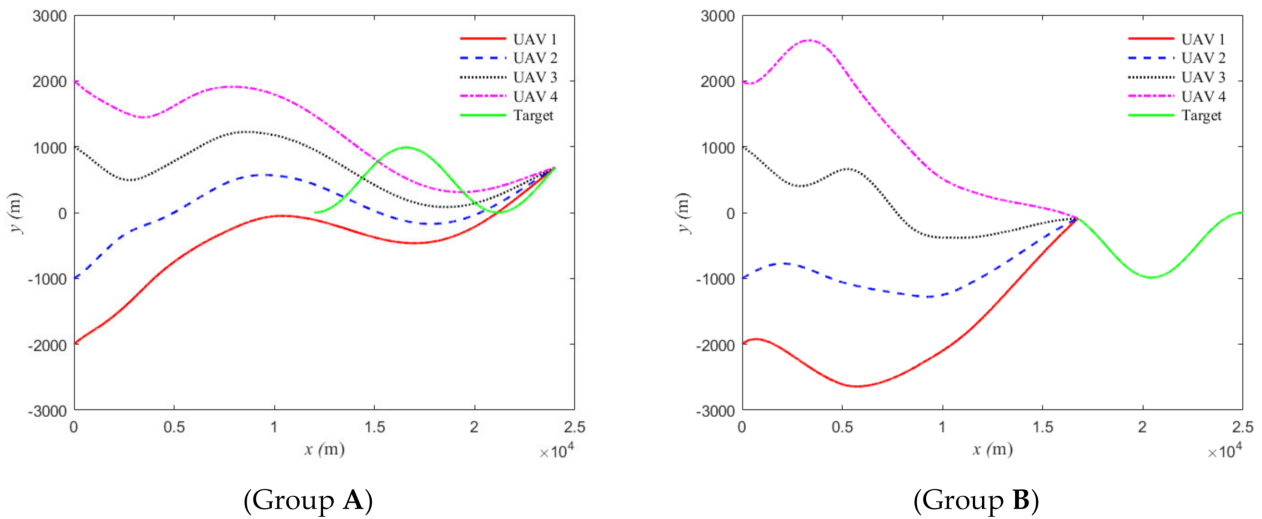
(Group **A**)   (Group **B**)

Figure 3. Trajectories of four UAVs to attack a maneuvering target simultaneously.
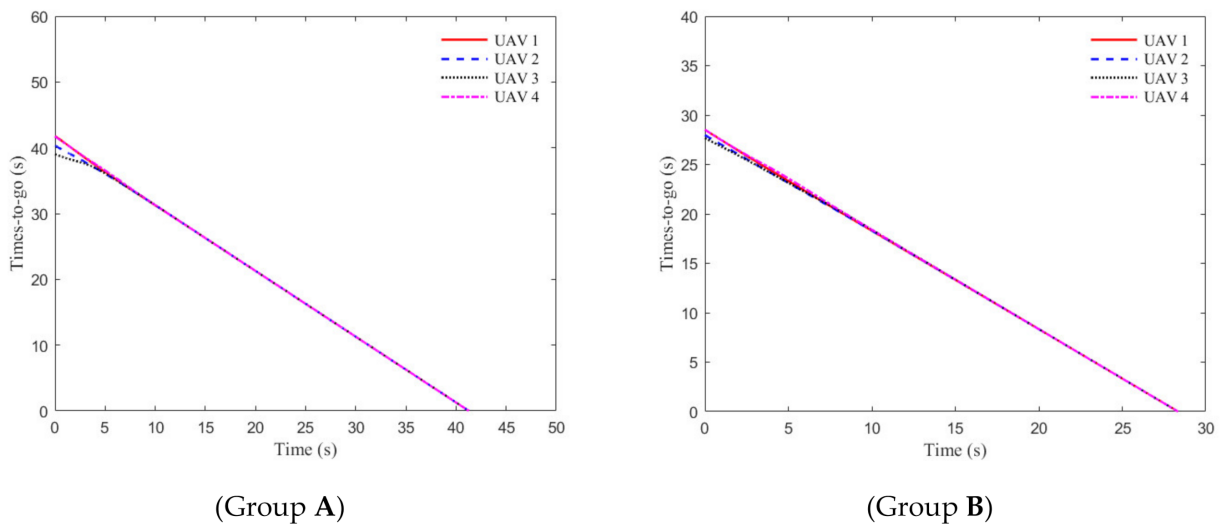
(Group **A**)   (Group **B**)

Figure 4. Time-to-go for four UAVs to attack a maneuvering target.
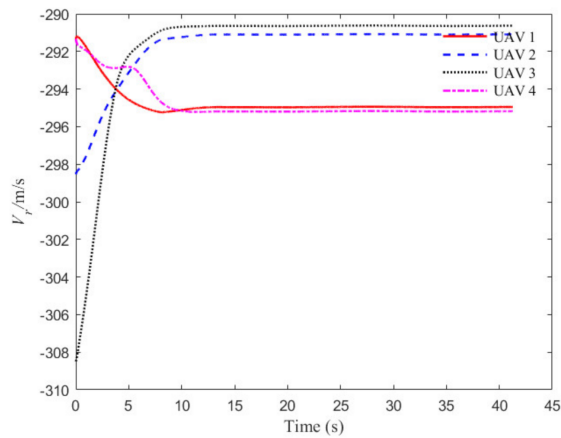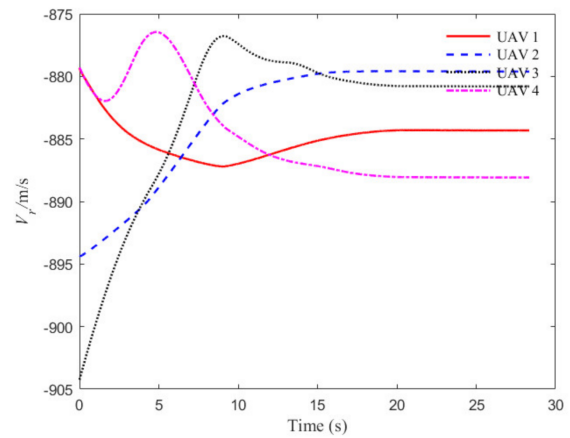
Figure 5. Radial relative velocities between four UAVs and a maneuvering target.
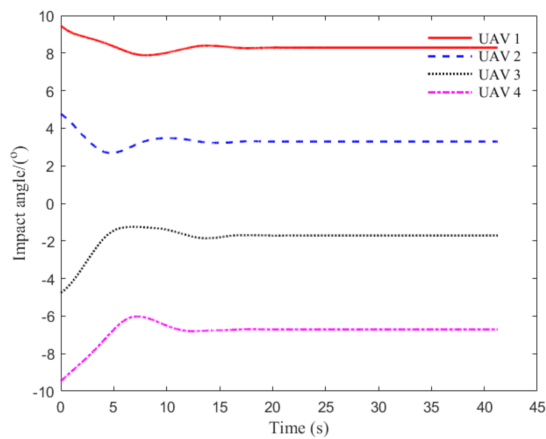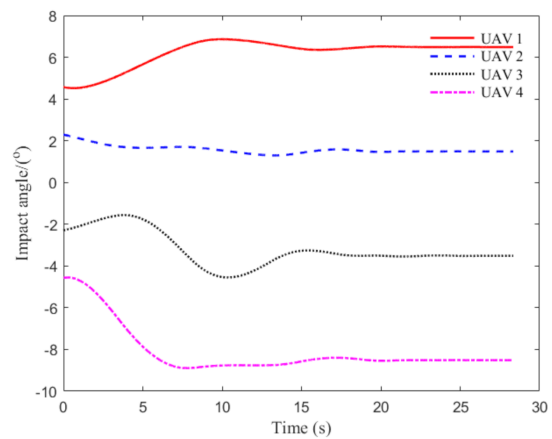
Figure 6. The impact angle of the UAVs.
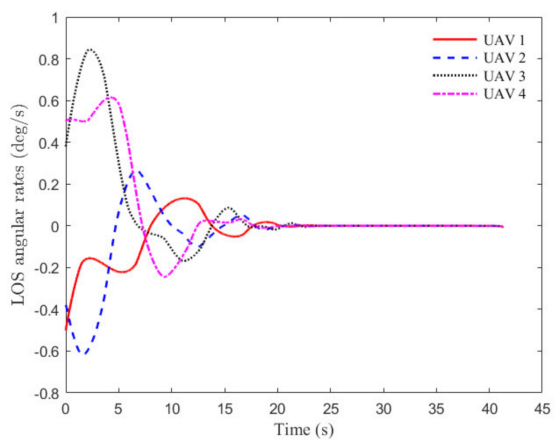
Figure 7. LOS angular rate of the UAVs.

(Group **A**)   (Group **B**)
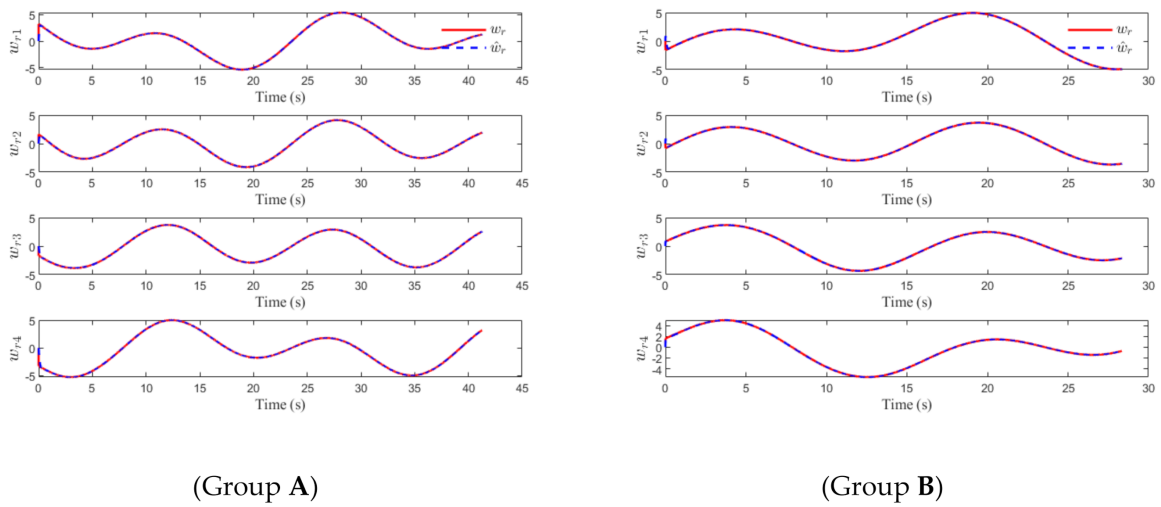
Figure 8. Actual and estimated values of external disturbance in the direction of LOS.

(Group **A**)   (Group **B**)
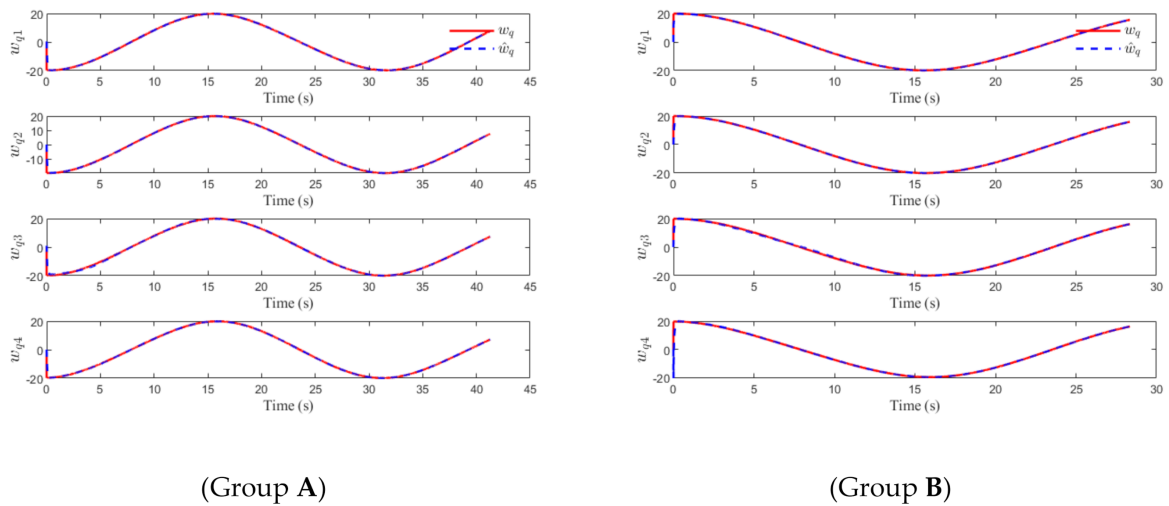
Figure 9. Actual and estimated values of external disturbance in the normal direction of LOS.

(Group **A**)   (Group **B**)
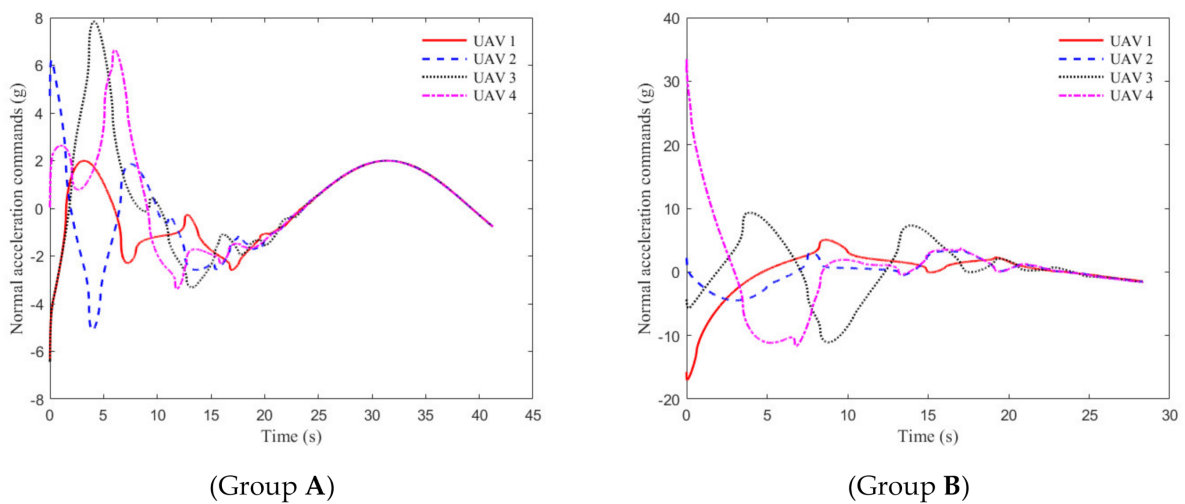
Figure 10. Normal overload commands.

In Figures 3 and 4, it can be seen that the four UAVs achieve a simultaneous attack on a maneuvering target. In addition, it can be observed in Figure 4 that the four UAVs

have different remaining flight times at moment zero. However, using the designed finite-time consensus protocol (34), the remaining flight time reaches the same value after approximately 10 seconds. Figure 5 shows that the relative velocity between the UAVs and the target converges to fixed values after some time. At the same time, the relative velocities of the different UAVs and the target do not converge to the same value, which avoids unnecessary energy consumption. Figures 6 and 7 indicate that under the angular cooperative guidance law (25), the LOS angle converges to the desired sequence after some time, while the LOS angle rate converges to zero.

As shown in Figures 8 and 9, the proposed FDO (15) has a favorable performance in estimating the disturbance caused by the unknown maneuvers of the target.

Figures 10 and 11 show that both the tangential acceleration commands and normal acceleration commands are smooth.

(Group **A**)   (Group **B**)
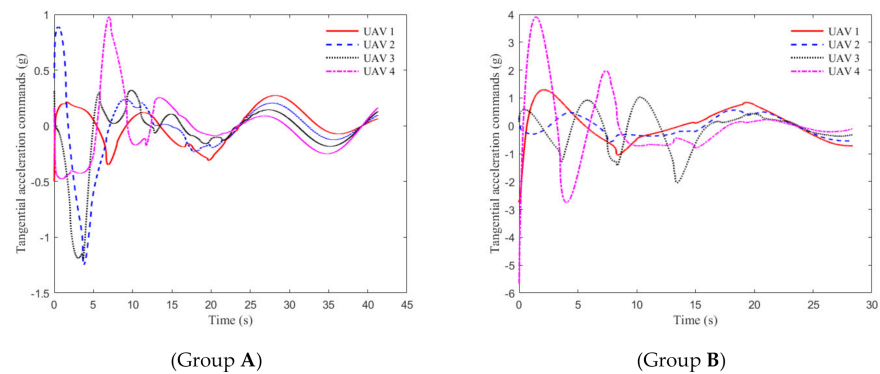
Figure 11. Tangential overload commands.

5.2. Comparison with Feedback Linearization Methods

We compared the tangential acceleration commands of the two methods for the initial condition A. From the Figure 12 we can see that the required overload command of the proposed method is significantly smaller. From the right-hand image, we can see that the required acceleration at the initial moment is large at around $4g$. At the same time, the acceleration required for the proposed method is less than $1g$. This is due to the fact that $\frac{r_i^2 \dot{q}_i^2}{\dot{r}_i^2}$ needs to be compensated directly in the feedback linearization method. Usually, $\dot{q}_i$ does not converge to zero at the initial moment and r_i is large at the same time, therefore resulting in a large overload command. At the same time, we can see that the feedback linearization method has a significantly higher acceleration command at the moment of hit. This is because the acceleration command includes $-\frac{r_i^2}{\dot{r}_i} \widetilde{u}_{ri}$. This leads that the overload command has critical singularities when $r_i \to 0$. Through comparison, it can be seen that the proposed method in this paper has a smaller overload command and is more promising for application.
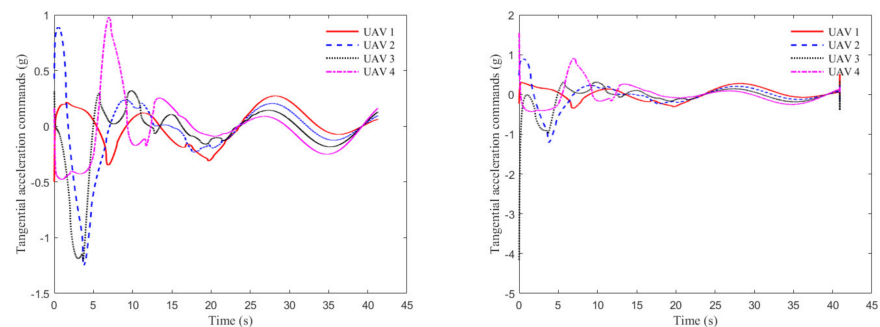
Figure 12. Comparison of overload commands.

6. Conclusions

This paper proposed a new cooperative guidance law that can be applied to targets with large maneuvers. We propose a new sliding mode FDO to estimate the rapidly changing acceleration of the target. Meanwhile, the guidance law was designed in two parts: angular cooperation and time cooperation to satisfy impact time and impact angle constraints. We adopt the nonlinear guidance law design to avoid numerical singularity caused by feedback linearization. A rigorous derivation demonstrates that the proposed guidance law can achieve a finite-time cooperative attack under directed communication topology. Numerical simulations show that the proposed guidance law could achieve a cooperative attack on a highly maneuverable target while avoiding the high tangential overload command of the UAVs. Future work will attempt to consider autopilot dynamics in the design of cooperative guidance law for actual engagement missions.

7. Annexes

A directed graph $\mathcal{G} = (\mathcal{V}, \mathcal{E})$ is developed for N agents to represent the interactions between agents, the vertex set and the edge set. Moreover, edges are an ordered pair of vertices $\mathcal{V}$, implying that agent j can receive information from agent i. If a directed edge from i to j exists, then i would be defined as the parent node, and j would be defined as the child node, the neighbors of node i are represented by $\mathcal{N}_i = \{j \in \mathcal{V} | (v_j, v_i) \in \mathcal{E}\}$ and $|\mathcal{N}_i|$ are the neighbor numbers of agent i.

The adjacency matrix A associated with $\mathcal{G}$ is defined such that $a_{ij} = 1$ if $i \neq j$ and node i is neighboring to node j, while $a_{ij} = 0$ otherwise. For a directed graph $\mathcal{G}$, $a_{ij} \neq a_{ji}$ and therefore the matrix A is asymmetric. The Laplacian matrix of the graph associated with adjacency matrix A is given as $\mathcal{L} = (l_{ij})$, where $l_{ii} = \sum\limits_{j=1}^{N} a_{ij}$ and $l_{ij} = -a_{ij}$, $i \neq j$.

Author Contributions: Writing—original draft X.D.; Writing—review & editing Z.R. All authors have read and agreed to the published version of the manuscript.

Conflicts of Interest: The authors declare no conflict of interest.

References

1. Jeon, I.S.; Lee, J.I.; Tahk, M.J. Impact-time-control guidance law for anti-ship missiles. *IEEE Trans. Control Syst. Technol.* **2006**, *14*, 260–266. [CrossRef]
2. Kim, M.; Jung, B.; Han, B.; Lee, S.; Kim, Y. Lyapunov-based impact time control guidance laws against stationary targets. *IEEE Trans. Aerosp. Electron. Syst.* **2015**, *51*, 1111–1122. [CrossRef]
3. Saleem, A.; Ratnoo, A. Lyapunov-based guidance law for impact time control and simultaneous arrival. *J. Guid. Control. Dyn.* **2016**, *39*, 164–173. [CrossRef]
4. Tekin, R.; Erer, K.S.; Holzapfel, F. Polynomial shaping of the look angle for impact-time control. *J. Guid. Control. Dyn.* **2017**, *40*, 2668–2673. [CrossRef]
5. Wang, Y.; Dong, S.; Ou, L.; Liu, L. Cooperative control of multi-missile systems. *IET Control Theory Appl.* **2014**, *9*, 441–446. [CrossRef]
6. Zhao, J.; Zhou, R. Obstacle avoidance for multi-missile network via distributed coordination algorithm. *Chin. J. Aeronaut.* **2016**, *29*, 441–447. [CrossRef]
7. Jiang, H.; An, Z.; Chen, S.; Xiong, F. Cooperative guidance with multiple constraints using convex optimization. *Aerosp. Sci. Technol.* **2018**, *79*, 426–440. [CrossRef]
8. Yao, Z.A.; St, B.; Jie, G.B. Two-stage cooperative guidance strategy using a prescribed-time optimal consensus method. *Aerosp. Sci. Technol.* **2020**, *100*, 105641.

9. Chen, Y.; Wang, J.; Shan, J.; Xin, M. Cooperative guidance for multiple powered missiles with constrained impact and bounded speed. *J. Guid. Control. Dyn.* **2021**, *44*, 1–17. [CrossRef]

10. Li, G.; Wu, Y.; Xu, P. Adaptive fault-tolerant cooperative guidance law for simultaneous arrival. *Aerosp. Sci. Technol.* **2018**, *82*, 243–251. [CrossRef]

11. Lyu, T.; Li, C.; Guo, Y.; Ma, G. Three-dimensional finite-time cooperative guidance for multiple missiles without radial velocity measurements. *Chin. J. Aeronaut.* **2019**, *32*, 241–251. [CrossRef]

12. Nikusokhan, M.; Nobahari, H. Closed-form optimal cooperative guidance law against random step maneuver. *IEEE Trans. Aerosp. Electron. Syst.* **2016**, *52*, 319–336. [CrossRef]

13. Zhao, J.; Zhou, R.; Dong, Z. Three-dimensional cooperative guidance laws against stationary and maneuvering targets. *Chin. J. Aeronaut.* **2015**, *28*, 1104–1120. [CrossRef]

14. Zhao, J.; Zhou, R. Unified approach to cooperative guidance laws against stationary and maneuvering targets. *Nonlinear Dyn.* **2015**, *81*, 1635–1647. [CrossRef]

15. Zhao, Q.L.; Dong, X.W.; Song, X.; Ren, Z. Cooperative time-varying formation guidance for leader-following missiles to intercept a maneuvering target with switching topologies. *Nonlinear Dyn.* **2019**, *95*, 129–141. [CrossRef]

16. Zhou, J.; Lü, Y.; Li, Z.; Yang, J. Cooperative guidance law design for simultaneous attack with multiple missiles against a maneuvering target. *J. Syst. Sci. Complex.* **2018**, *31*, 287–301. [CrossRef]

17. Shaferman, V.; Shima, T. Cooperative optimal guidance laws for imposing a relative intercept angle. *J. Guid. Control Dyn.* **2015**, *38*, 1395–1408. [CrossRef]

18. Shaferman, V.; Shima, T. Cooperative differential games guidance laws for imposing a relative intercept angle. *J. Guid. Control Dyn.* **2017**, *40*, 2465–2480. [CrossRef]

19. Wang, X.H.; Tan, C.P. 3-D impact angle constrained distributed cooperative guidance for maneuvering targets without angular-rate measurements. *Control Eng. Pract.* **2018**, *78*, 142–159. [CrossRef]

20. Yu, J.; Dong, X.; Li, Q.; Ren, Z. Distributed cooperative encirclement hunting guidance for multiple flight vehicles system. *Aerosp. Sci. Technol.* **2019**, *95*, 105475. [CrossRef]

21. Wang, X.; Zhang, Y.; Liu, D.; He, M. Three-dimensional cooperative guidance and control law for multiple reentry missiles with time-varying velocities. *Aerosp. Sci. Technol.* **2018**, *80*, 127–143. [CrossRef]

22. Chen, Z.Y.; Chen, W.C.; Liu, X.M.; Cheng, J. Three-dimensional fixed-time robust cooperative guidance law for simultaneous attack with impact angle constraint. *Aerosp. Sci. Technol.* **2021**, *110*, 106523. [CrossRef]

23. Liu, F.; Dong, X.; Li, Q.; Ren, Z. Robust multi-agent differential games with application to cooperative guidance. *Aerosp. Sci. Technol.* **2021**, *111*, 106568. [CrossRef]

24. Lin, M.; Ding, X.; Wang, C.; Cui, N. Fixed-time cooperative guidance law with angle constraint for multiple missiles against maneuvering target. *IEEE Access* **2020**, *1*, 99.

25. Song, J.; Song, S.; Xu, S. Three-dimensional cooperative guidance law for multiple missiles with finite-time convergence. *Aerosp. Sci. Technol.* **2017**, *67*, 193–205. [CrossRef]

26. Zhai, S.; Wei, X.; Yang, J. Cooperative guidance law based on time-varying terminal sliding mode for maneuvering target with unknown uncertainty in simultaneous attack. *J. Frankl. Inst.* **2020**, *357*, 11914–11938. [CrossRef]

27. Bhat, S.; Bernstein, D. Finite time stability of continuous autonomous systems. *SIAM J. Control Optim.* **2000**, *38*, 751–766. [CrossRef]

28. Zuo, Z.; Tie, L. Distributed robust finite-time nonlinear consensus protocols for multi-agent systems. *Int. J. Syst. Sci.* **2016**, *47*, 1366–1375. [CrossRef]

29. Ran, M.; Wang, Q.; Dong, C. Stabilization of a class of nonlinear systems with actuator saturation via active disturbance rejection control. *Automatica* **2016**, *63*, 302–310. [CrossRef]